Icarus 394 (2023) 115416

Contents lists available at ScienceDirect

Icarus

journal homepage: www.elsevier.com/locate/icarus

Martian dust storm distribution and annual cycle from Mars daily global map observations

Huiqun Wang [a,*], Morgan Saidel [b], Mark I. Richardson [c], Anthony D. Toigo [d], J. Michael Battalio [e]

[a] Smithsonian Astrophysical Observatory, Harvard-Smithsonian Center for Astrophysics, Cambridge, MA, USA
[b] Division of Geological and Planetary Sciences, Californian Institute of Technology, Pasadena, CA, USA
[c] Aeolis Research, Chandler, AZ, USA
[d] John Hopkins University Applied Physics Laboratory, Laurel, MD, USA
[e] Dept. Earth & Planetary Sci., Yale University, New Haven, CT, USA

ARTICLE INFO

Keywords:
Mars, atmosphere
Mars, climate
Mars
Atmospheres, composition
Meteorology

ABSTRACT

Dust storms were manually tracked in Mars Reconnaissance Orbiter (MRO) Mars Daily Global Maps (MDGMs) from Mars Year 29 to 33. The data were used to construct the Mars Dust Storm Sequence Dataset (MDSSD), which contains >12,000 dust storm instances that are distinguishable from the ubiquitous dust background. Based on the dust storm climatology, we propose a partition of a Mars year into six pseudo-seasons or "sextons" (named "Unober", "Duober", "Triober", "Quartober", "Quintober", and "Sixtober", respectively). The greatest dust storm activity is observed in the 3rd, 4th and 6th sextons (Triober, Quartober and Sixtober), with each containing one or more dust storm episodes. We also propose a hierarchical system for organizing information and describing the process through which dust storms develop. The hierarchy of storm behavior is described in terms of dust storm episodes within these sextons, with each episode being composed of one or more dust storm sequences, and with each dust storm sequence being composed of multiple dust storm members.

The occurrence of a large dust storm episode typically results from multiple dust storm sequences that are simultaneous, staggered, or merged, though one of the component sequences typically plays a dominant role. The typical evolutionary pathway through which a large dust storm sequence develops consists of dust activity progressing from the northern to the southern hemispheres, with multiple flushing dust storm members in the northern hemisphere and followed by a much larger zonally extended dust storm member in the southern hemisphere. Differences among Mars years are related to the timing, order, and trajectories of dust storm sequences, though the overall spatial coverage of dust storm instances within a sexton is similar across years. A striking characteristic of Martian dust storm distribution is the quasi-periodic recurrence exhibited by dust storm episodes and dust storm sequences.

1. Introduction

Martian dust storms can attain a large scale, with some storms occupying a wide latitudinal band, longitudinal channel, or even enshrouding the whole planet. The close coupling between the dust distribution and the atmospheric circulation is a fundamental aspect of Martian weather and climate. In particular, large dust storms exhibit prominent optical, thermal, and dynamical signatures in the Martian atmosphere (Kahre et al., 2017; Barnes et al., 2017). Strikingly, the mechanisms of large storm growth and development remain poorly understood. It is therefore important to illustrate the characteristics of dust storm distributions both as a basis for determining the mechanisms of storm development and also for understanding the impacts of major storms on the Martian climate. General reviews of spacecraft observations of dust activity and dust optical depth can be found in, e.g., Smith (2008), Montabone et al. (2015), Kahre et al. (2017). Here, we focus on the aspects that are pertinent to this paper.

The systematic coverage provided by Mars Daily Global Maps (MDGMs) created from both the Mars Global Surveyor (MGS) Mars Orbiter Camera (MOC) and the Mars Reconnaissance Orbiter (MRO) Mars Color Imager (MARCI) (Wang and Ingersoll, 2002; Cantor, 2007; Wang and Gonzalez Abad, 2021) offers a unique opportunity to study

Abbreviations: MDSSD, Mars Dust Storm Sequence Dataset; MDGM, Mars Daily Global Map; MDAD, Mars Dust Activity Database.

* Corresponding author.
E-mail address: hwang@cfa.harvard.edu (H. Wang).

https://doi.org/10.1016/j.icarus.2022.115416
Received 23 June 2022; Received in revised form 18 December 2022; Accepted 21 December 2022
Available online 25 December 2022

the statistical distribution and developmental histories of various dust storms. Previous studies revealed a concentration of dust storms near the polar caps and within certain longitudinal corridors at lower latitudes, an overall trend of increased size and occurrence frequency during the dust storm season (roughly southern spring and summer), and a local minimum in dust storm activity near each hemisphere's winter solstices (Cantor et al., 2001; Cantor, 2007; Wang and Richardson, 2015; Guzewich et al., 2015, 2017; Battalio and Wang, 2021).

The classification of dust storms is not standardized, however. Martin and Zurek (1993) provided a widely used scheme for Martian dust storms using historical observation records, where a "local" dust storm has a long axis of <2000 km, a "planet-encircling" dust storm completely occupies a latitudinal band, and a "regional" dust storm has an intermediate size. In this terminology, a "great" or "global" dust storm (GDS) that covers most or all of the planet fits into the largest planet-encircling dust storm category. Cantor et al. (2001) refined this classification scheme by defining a "regional dust storm" as having an area $> 1.6 \times 10\ \mathrm{km}^2$ and a duration >3 sols (Mars days), which is useful for describing dust storms observed in spacecraft images.

As large dust storms typically result from the aggregation of smaller storms over time (Zurek and Martin, 1993; Cantor et al., 2007), Wang and Richardson (2015) introduced the term "dust storm sequence" to describe the process through which a large dust storm develops. A dust storm sequence consists of a series of dust storm members (i.e., individual local and/or regional dust storms as defined by Cantor et al., 2001) that appear to be organized so as to maintain continuous activity along an identifiably coherent spatial trajectory during the sequence lifetime. Using this concept, Battalio and Wang (2021) compiled a comprehensive Mars Dust Activity Database (MDAD) where individual dust storms were tracked throughout their lifetimes and dust storm members were grouped into dust storm sequences when appropriate. An individual dust storm is a "member" if there is a sequence to which the individual dust storm belongs. Individual dust storms not belonging to a sequence are just isolated storms (note that there is a slight difference in terminology between this paper and Battalio and Wang, 2021, see the Appendix). Their results show that the trajectories exhibited by dust storm sequences frequently originate from the Acidalia, Utopia, Argyre-Solis-Valles Marineris (ASV), Noachis-Hellas, Arcadia, and Cimmeria-Sirenum (CS) regions.

Large dust storms typically generate pronounced atmospheric thermal signatures. Using these thermal signatures, Kass et al. (2016) defined "large regional" dust storms as those associated with a zonal mean temperature at 50 Pa exceeding 200 K, and classified pre-, near and post- perihelion storms as "A", "B" and "C" storms for Mars years without a GDS. Besides these southern spring and summer storms, dust storms in late northern summer can occasionally produce significant thermal perturbations, with ASV-originated storms being particularly noticeable (Battalio and Wang, 2019; Steele et al., 2021). Heavens et al. (2019) identified them as "Z" storms. It turns out that the combined seasonal coverage of the "Z", "A", "B", and "C" storms roughly spans the conventional "dust storm season" (solar longitude $L_S = 160° – 330°$) as defined in Martin and Zurek (1993).

The terminology developed for Martian dust storms thus depends on the type of measurement used and/or on the user application. Without context, the variety of terminology and classification may be confusing. For example, while the "regional dust storm" designation implies that a certain size requirement has been met, it is difficult to tell whether it refers to a single dust storm instance (a data object) identified in an image, a trackable individual dust storm throughout its lifetime, a member of a dust storm sequence, or the final product of a series of dust storm members and/or dust storm sequences. Furthermore, some dust storms of regional size exist outside the dust storm season and have little influence on atmospheric temperature at 50 Pa; in contrast, "B" storms that are typically small in area are associated with a pronounced signal in temperature observations (Battalio and Wang, 2021; Kass et al., 2016). Identification of storms through temperature signatures (and/or in other meteorological variables) may not always correspond to a visible image dust storm occurrence (Martinez-Alvarado et al., 2009; Battalio and Wang, 2020). Thus, classifications using atmospheric temperature and storm area are different and reflect different aspects of the dust storms they designate.

In this paper, we develop a system to organize information on the spatio-temporal distribution of dust storms observed in MDGM images. The system captures the styles of dust storm evolution throughout a typical Mars year. We describe the data and methods used in this paper in Section 2. In Section 3, we introduce additional terms used to describe Martian dust storms, explain the relationships among the terms, and illustrate the differing behavior of dust storms over the annual cycle. A glossary can also be found in the Appendix for reference. While our designations do not provide the only way to explore and categorize the data, they mitigate confusion, and we hope they will at a minimum inspire even more useful perspectives in future works.

2. The Mars Dust Storm Sequence Dataset (MDSSD)

The 0.1° longitude x 0.1° latitude Version 2.1 color Mars Daily Global Maps (MDGMs) (Wang and Gonzalez Abad, 2021) are used to compile the dust storm data used in this study. The MDGMs were made from the wide-angle global map swaths taken by MARCI (Bell III et al., 2009; Malin et al., 2001) on board the MRO spacecraft (Zurek and Smrekar, 2007). The raw images were processed through radiometric calibration and photometric correction. Each MDGM is the result of merging 13 consecutive sets of processed MARCI images taken around 3 PM local time over approximately one sol. MDGMs were intended to facilitate global visualization of dust storms and water ice clouds. The MDGMs examined for this study cover the time period from Mars year (MY) 29 to 33 (images taken from December 2007 to May 2017). Due to the better spatial resolution and the daily cadence of effectively global coverage with the MDGMs, dust storm catalogs (such as that described in this paper) resolve much more detail of the development of dust storms, as compared to those derived from other datasets, such as the MRO Mars Climate Sounder and MGS Thermal Emission Spectrometer retrievals (e.g., Liu et al., 2003; Smith, 2004; Montabone et al., 2015; Kass et al., 2016).

We manually identify the borders of each dust cloud identified in each MDGM based on its distinct color, morphology, and texture (Guzewich et al., 2015, 2017; Kulowski et al., 2017). We call them *dust storm instances* following Battalio and Wang (2021). A dust storm instance is an instantaneous "snapshot" of an individual dust storm. If an instance is the first detection of a given individual dust storm (i.e., there was no related instance on the prior sol), then a new and unique Storm ID is generated and the instance is tagged with this Storm ID. If instead, the instance is an apparent continuation of an individual dust storm from the prior sol, the instance inherits the same Storm ID tag as that of the prior sol instance. In this way, two or more objects in a time sequence may have the same instance Storm ID if they appear to be images of the individual dust storm over two or more sols. Each individual dust storm is then a single dust cloud that has been seen over one or more sols. The storm ID is used to track an individual dust storm throughout its lifetime.

Some larger dust storm systems are composed of many different individual dust storms that overlap in time. These larger storm systems are called "dust storm sequences". If an individual dust storm is deemed to be a part of a dust storm sequence, it is called a "dust storm member" of that sequence. Each dust storm instance of each individual dust storm in the sequence is then additionally tagged with a unique "Sequence ID" which represents the whole sequence. Thus, a dust storm sequence is a collection of dust storm members that are seemingly organized by following an identifiable trajectory and displaying a coherent development history (Wang and Richardson, 2015; Battalio and Wang, 2021). Note that Battalio and Wang (2021) refers to all individual dust storms as dust storm members, but in this paper, dust storm members are a subset of individual dust storms that belong to a dust storm sequence. See the Appendix for additional description of the terms.

The MDAD v1.0 (Battalio and Wang, 2021) contains all the dust storm instances identified in the Mars Global Surveyor (MGS) MDGMs and the Version 2.0 Mars Reconnaissance Orbiter (MRO) MDGMs, covering the time period from MY 24 $L_s = 150^\circ$ to MY 32 $L_s = 171^\circ$. The MDAD also tracked dust storm sequences that lasted longer than 3 sols. Using MDAD as a starting point, we revisited and reviewed a large portion of the existing MRO data in MDAD v1.0, while also collecting new data for the remainder of MY 32 and for MY 33. During the review and data collection, we focused on the sols that were part of large dust storm sequences, though dust storm instance data on other sols were also occasionally collected along the way. Note, on all the sols we examined, data are collected for both non-sequence individual dust storms and dust storm members when they existed. During the review process, we updated (split, merged, changed), deleted, or added dust storm instances boundaries, and modified their storm IDs and sequence IDs as appropriate. We call the resulting dataset the Mars Dust Storm Sequence Dataset (MDSSD).

For convenience of presentation in this paper, we divided the Martian surface into six large regions (Fig. 1) according to the origination areas of the frequently observed large propagating dust storm sequences (i.e., regions where dust storm members are observed on their first sol). We use the names of these regions to refer to dust storm instances, individual dust storms and dust storm sequences in subsequent descriptions. For example, an “Acidalia sequence” is one that initiates from the Acidalia region as defined in Fig. 1 and propagates through this region. It remains an “Acidalia sequence” even if other dust storm members of the sequence were to occur on subsequent sols outside the Acidalia region. Sometimes, multiple dust storms occur daily around the polar regions with no significant equatorward excursion nor global impact on atmospheric circulation, e.g., the formation of the polar hoods or the spring and summer-time polar cap edge population. These were often grouped as circumpolar sequences in MDAD v1.0. For MDSSD, although we recorded some circumpolar individual dust storms, they are not the focus of this study, and thus we did not attempt to identify all such circumpolar sequences and only occasionally assigned sequence IDs for these polar dust storms.

The MDSSD contains >12,000 dust storm instances of which >7000 are individual dust storms that have unique storm IDs (Note that each multi-sol individual dust storm retains its storm ID throughout its lifetime, and the storm ID of each single-sol individual dust storm only appears once in the MDSSD), and >200 dust storm sequences collected from over 2000 MDGMs. Note that the storm IDs and sequence IDs are meant to be self-consistent within the MDSSD only. Thus, even if an ID is

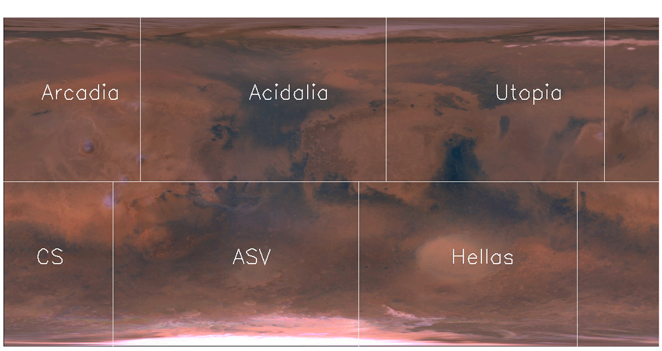

Fig. 1. The named regions used to categorize the origination locations of dust storm instances, individual dust storms and dust storm sequences in this paper. The names are meant to be indicative of the overall regions rather than representing exact cartographical areas on Mars. The Arcadia, Acidalia, and Utopia regions in the northern hemisphere are bordered by 105°W, 30°E, and 150°E. The Cimmeria-Sirenum (CS), Argyre-Solis-Valles Marineris (ASV), and Hellas regions in the southern hemisphere are bordered by 120°W, 15°E, and 135°E.

present in both the MDSSD and MDAD, it may sometimes refer to a different individual dust storm. The identified dust storm instances in each MDGM are with respect to the surrounding dust background which can have either low or high optical depth. For example, there are no dust storm instances when only a large-scale dust haze (without a clear boundary) is present in a MDGM. In the MDSSD, we do not count the fully developed polar hood (which may involve both dust and condensates) as an individual dust storm, nor do we count any long streaks inside the polar hood. However, we identify the individual dust storms that lead to the polar hood formation and the individual dust storms that stand out against or extend beyond the fully developed polar hood.

Fig. 2 shows examples of the MDSSD data for six consecutive sols. Non-sequence individual dust storms are marked in white. Dust storm members of an Acidalia sequence, a Utopia sequence, and an ASV sequence are marked in green, yellow and blue, respectively. Clearly, it is possible for there to be one or more dust storm sequences on any individual sol. For each dust storm sequence, dust storm members can occur anywhere along the sequence trajectory and anytime during the sequence development, but there can be no break in dust activity along the trajectory during the sequence lifetime. There can be one or more dust storm members of the corresponding sequence on each sol. A dust storm member can be of any size and duration and is an integral part of the dust storm sequence.

A 4-tier confidence level is used to record the data collector’s subjective assessment of the data quality, with a level of 4 being the best. A level of 3 or 4 implies that a dust storm instance is easily distinguishable from the background along most or all of its boundary, while a confidence level of 1 signifies that most of the boundary is diffuse and difficult to determine even though a dust opacity anomaly seems to be present. A confidence level of 1 is also used when an identified instance is suspected to be a dust storm but may not actually be one due to the residual image processing artifacts in MDGMs. In MDSSD, a large-scale dust haze is considered to be the dust background of the general region instead of a dust storm instance. The qualitative difference between level 1 and level ≥ 3 is usually clear (Fig. 2 dotted and solid lines) and the difference between level 1 and level 2 (dashed) is moderate. In the MDSSD, about 14% of the dust storm instances have a confidence level of 1.

Due to the nature of the collected data, differences are inevitable between the MDAD and MDSSD. The differences result partly from the version of MDGMs used, partly from human errors, and partly from the data collectors’ differences of opinion on dust storms boundaries, durations, and sol-to-sol movement. Typically, dust storm instances with thick optical depth, distinctive texture and/or sharp boundary belong to the top two confidence levels and agree well between both datasets. However, dust storm instances with lower confidence levels can have substantial differences. These are typically caused by diffuse boundaries, faint optical depth anomalies, and the extreme observational geometries of wide-angle images (e.g., near the seams between adjacent MARCI swaths in a MDGM). Some difficulties are related to the limitations of MARCI observations, as the pixels with extreme geometries are difficult to process in MDGMs, and the once per day revisit time prevents continuous feature tracking. The results for those cases are based on our best effort. Overall, the L_S versus latitude distribution of the dust storm instances in MDSSD (Figs. 3 and 4) strongly resembles that in MDAD v1.0 (compare with Fig. 2 of Battalio and Wang, 2021). The overall resemblance between the two datasets also extends to the distribution of dust storm locations (Supplementary Fig. S1) and sizes (Supplementary Fig. S2). The MDSSD appears to have more dust storm instances with smaller areas, possibly because some large dust storm instances in the MDAD were broken into smaller ones in MDSSD upon further inspection.

Despite the qualitative nature and caveats associated with the MDSSD, the fundamental principle of extracting useful information from imperfect data is applicable to almost all real-world datasets. This type of data provides a unique perspective through daily global observation and contains valuable information on dust storm development history

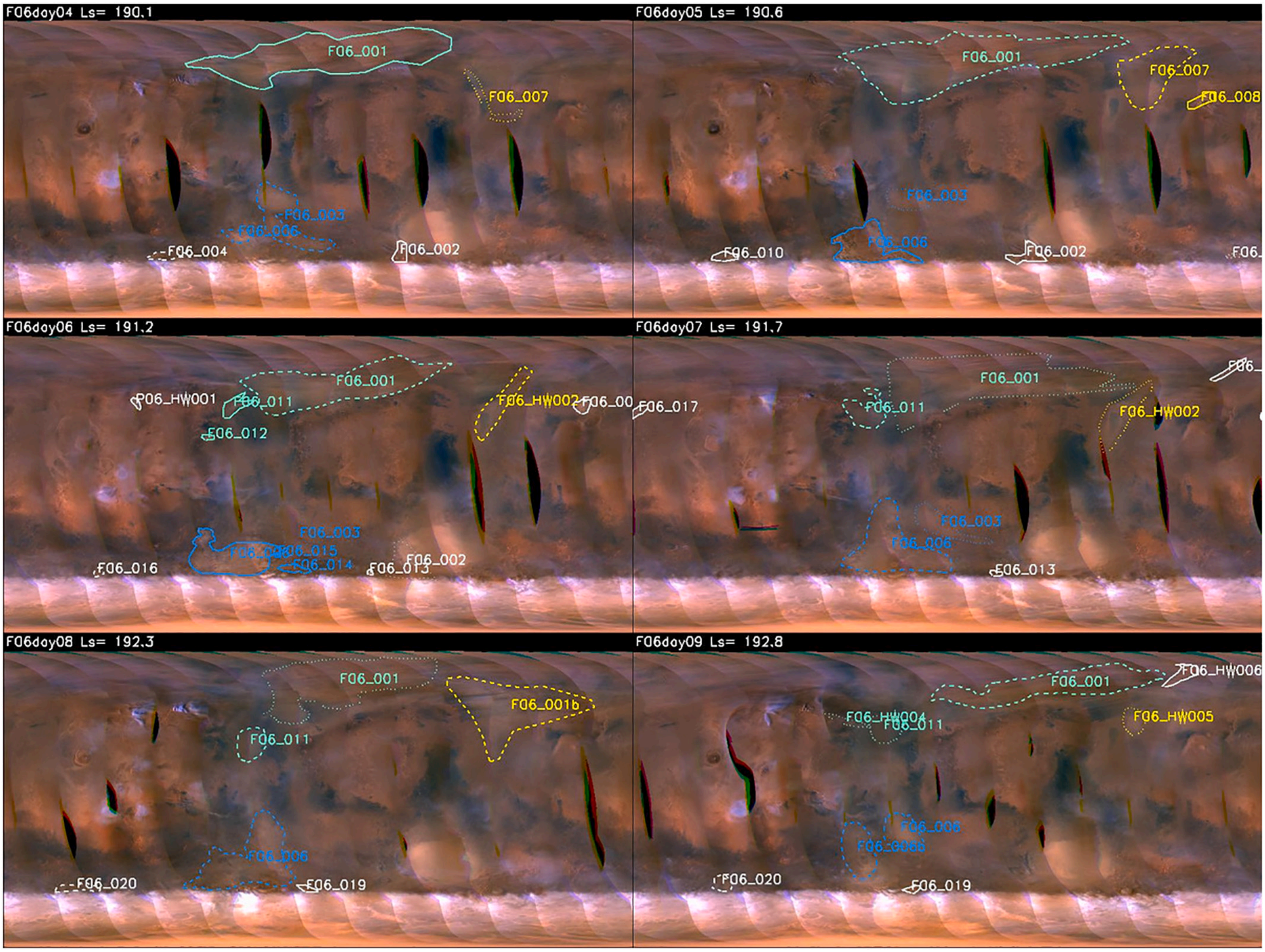

Fig. 2. MDSSD individual dust storms and dust storm sequences identified in six consecutive MDGMs during $L_s = 190.1°–192.8°$ of MY 32 (from left to right on each row and then rows from top to bottom). The MDGM name is indicated in the upper left corner of each panel. For each individual dust storm the enclosing boundary is shown, and it is labeled with the Storm ID. Solid lines correspond to a confidence level of 3 or 4, dashed lines correspond to a confidence level of 2, and dotted lines to a confidence level of 1. White lines indicate non-sequence individual dust storms. Other colors indicate dust storm members of dust storm sequences, with the Acidalia sequence (Sequence ID: F06_HW01) in green, the Utopia sequence (Sequence ID: F06_HW02) in yellow, and the ASV sequence (Sequence ID: F06_01) in blue. Note, an ID name is merely an arbitrary label assigned to an individual dust storm or a dust storm sequence, and the characters used in the name do not imply any specific organizationally coded meaning. (For interpretation of the references to color in this figure legend, the reader is referred to the web version of this article.)

and distribution. In this paper, we strive to present statistically robust patterns derived from the MDSSD. To this end, we emphasize the daily accumulated dust storm area rather than the area of individual dust storm, as the former depends less on the details of the boundaries of dust storm instances and some error cancellation among them is expected. The scientific conclusions presented in this paper are not sensitive to the inclusion or exclusion of the lowest confidence-level storms in the analyses.

3. Results

3.1. *Latitude versus time distribution of dust storm instances*

Fig. 3 shows the latitude versus L_s distribution of the dust storm instances observed in MDGMs from MY 29 to 33. The background shading represents the zonal mean dust optical depth derived from the Montabone et al. (2015) dust scenario (scaled to the 610 Pa level). Each circle is proportional to the area of the dust storm instance and plotted using the centroid latitude and MDGM's L_s value. The color of each circle represents the geographical region (Fig. 1) where the centroid is located. The bars at the bottom and top of each panel indicate whether the data come from the MDSSD (black, whether they are present in the MDAD v1.0 or not) or the MDAD v1.0 only (yellow), or whether the data have not been examined for any dust storm instances (gray). The time periods when MDGMs are unavailable are indicated by hatches. As mentioned earlier, data collected in the MDSSD mainly focuses on the time periods where dust storm sequences occur. For the time periods where dust storm sequences were not observed, data were either taken directly from the MDAD v1.0 or were just not collected.

The distribution in Fig. 3 exhibits previously recognized general behaviors, including the existence of a "dust storm season," the tendency of dust storm instances to follow the polar caps, the "solsticial pauses" in both hemispheres, and the occasional excursions of dust activity towards the low latitudes and beyond (Martin and Zurek, 1993; Cantor et al., 2001, 2007; Wang and Richardson, 2015; Guzewich et al., 2015; Battalio and Wang, 2019, 2021).

Fig. 3 shows that the dust storm instances are generally larger during the dust storm season than the rest of the year. In addition, all the large dust optical depth increases are immediately preceded by clusters of relatively large dust storm instances ($> 5 \times 10^6$ km^2). In other words,

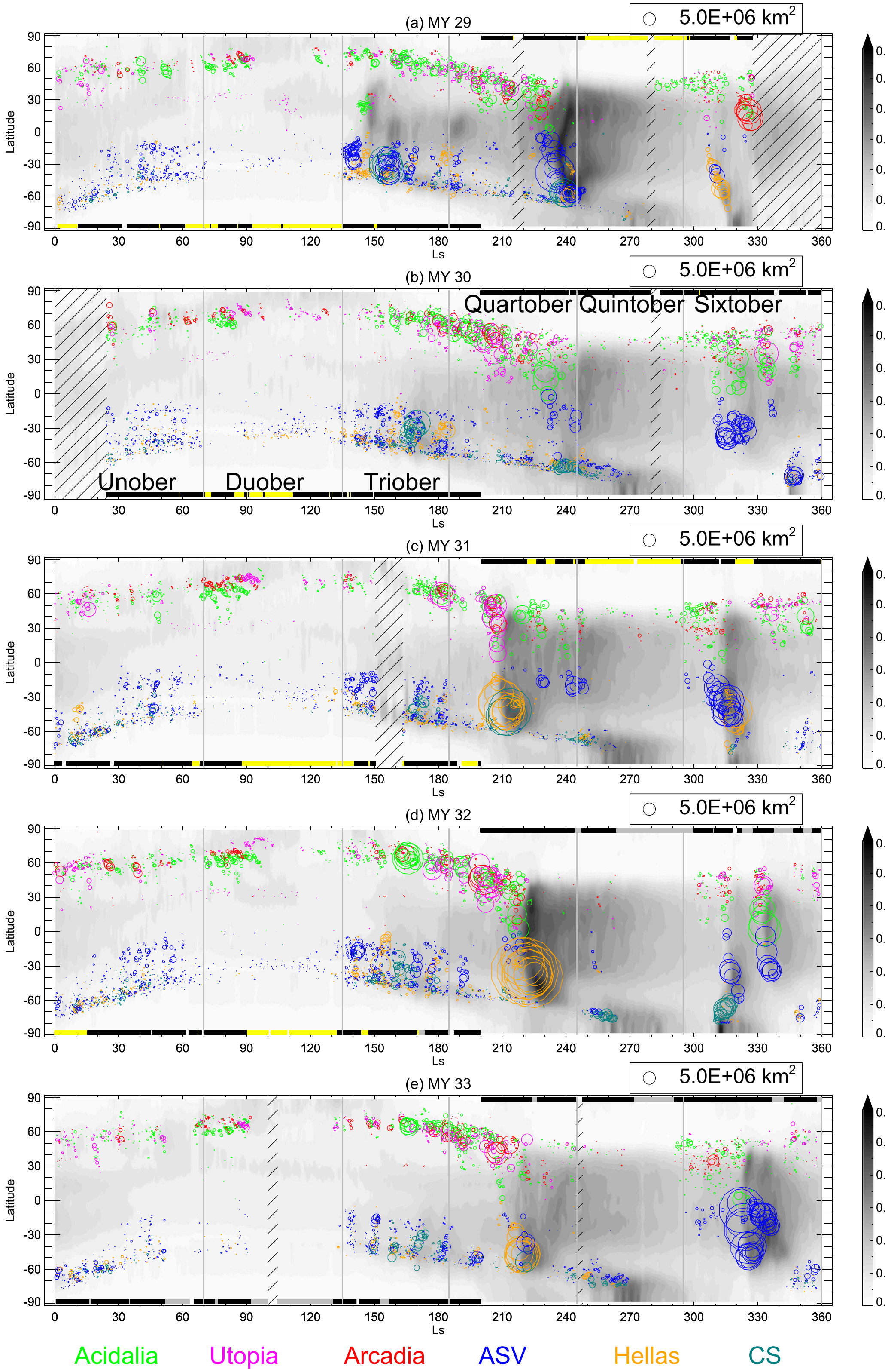

Fig. 3. Latitude versus L_s distribution of dust storm instances for (a-e) MY 29–33. Background shading indicates the zonal mean IR column dust optical depth (scaled to 610 Pa) derived from Montabone et al. (2015) dust scenarios. Each circle represents a dust storm instance, symbol size is proportional to the instance's area and color represents the region where the centroid is located (Fig. 1). Hatches indicate time periods of missing MDGMs. Bars at the bottom and top of each panel indicate whether the data come from MDSSD (black, regardless of whether the day is present in MDAD v1.0 or not), MDAD v1.0 only (yellow) or have not been examined (gray). Vertical gray lines delimit the 6 sextons, with their names denoted in Panel (b). (For interpretation of the references to color in this figure legend, the reader is referred to the web version of this article.)

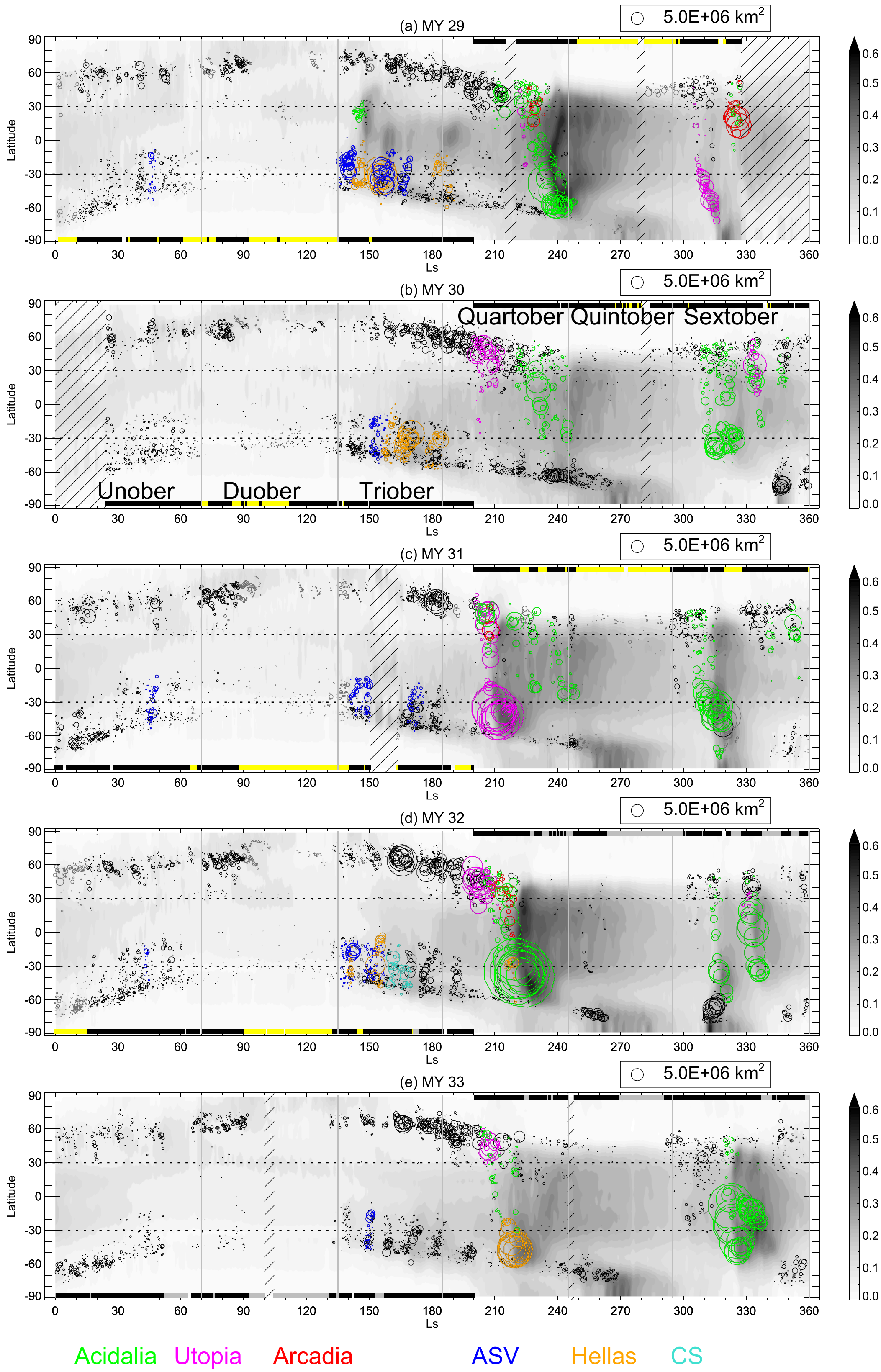

Fig. 4. The same as Fig. 3, but the dust storm instance symbols are colored according to the origination regions of their corresponding dust storm sequences. Only the dust storm instances belonging to dust storm sequences that occupy an area $> 2 \times 10^6$ km^2 within 30°S–30°N (between the dotted lines) at any point during the sequence development histories are colored according to the legend at the bottom. Other dust storm instances are colored in either black (MDSSD) or gray (MDAD v1.0).

these are the members of the dust storm sequences that lead to the large increase in background dust opacity. Note that the identification of dust storm instances depends on visual anomalies with identifiable boundaries over the dust background. With the increase of large-scale background dust opacity, dust storm instance boundaries usually become blurrier and eventually just merge into the background.

Dust storm instances observed at high latitudes occur at all longitudes as shown by the different colors in Fig. 3. They scatter around the polar cap, implying the effect of the baroclinic zone in the vicinity of the polar caps and/or polar vortices. When these cap edge individual dust storms are grouped into north/south polar sequences, the corresponding sequences tend to have extra-long durations with small peak areas, as the individual dust storms are confined in the polar regions and the cap edge dust activity can last up to a couple tens of degrees of L_s. However, the spatio-temporal distribution of these high latitude cap edge individual dust storms can be illustrated in Fig. 3 without any reliance on circumpolar sequence ID assignment.

The dust storm instances at lower latitudes in each hemisphere often reside in a main region for each episode, with occasional additions from the other regions in the corresponding hemisphere. As will be explained next, these dust storm instances are related to the individual dust storms that tend to organize into longitudinally propagating dust storm sequences trackable from the source to destination regions along their trajectories. They are the agents that primarily control the variations in large-scale dust opacity.

3.2. Latitude versus time distribution of dust storm sequences

Fig. 4 shows the same data as those in Fig. 3 except that the dust storm instances are now color coded to indicate their associated dust storm sequence, when appropriate. Specifically, the dust storm sequences that occupy an area $> 2 \times 10^6$ km^2 within 30°S–30°N (between the dotted lines) at any point during their development histories are colored according to their origin regions. This selection criterion singles out the dust storm sequences that have the potential to influence the large-scale background dust opacity. The origination regions include Acidalia, Utopia, and Arcadia in the northern hemisphere, and ASV, Hellas, and CS in the southern hemisphere, as defined in Fig. 1. As pointed out in other work (Wang and Richardson, 2015; Battalio and Wang, 2021), large dust storm sequences most frequently originate from Acidalia in the northern hemisphere and from ASV in the southern hemisphere. Note that dust storm members identified on any sol after the initial sol of the sequence may occur in regions other than that of the sequence origination region.

With the exception of a few relatively small southern hemisphere cases during $L_s = 30°$–$60°$, all the other colored dust storm sequences occur during the dust storm season. Most of the dust storm sequences during $L_s = 185°$–$360°$ are associated with northern hemisphere origins and the dust activity shifts with time to the southern hemisphere, sometimes even continuing to the south polar region. The northern fall of MY 33 is special as the dust storm members near Hellas were not traced back to an origin in the northern hemisphere. However, a small Acidalia sequence crossed the equator and overlapped in duration with the Hellas sequence. Further discussions about the dust storm sequences in northern fall and winter is presented in Section 3.4. The southern hemisphere dust storm sequences during $L_s = 135°$–$185°$ are intermediate in size. Among them, the ones in MY 29 are particularly noticeable. They are associated with significant increase in the zonal mean dust opacity (Fig. 4) and changes in atmospheric circulation (Montabone et al., 2015; Battalio and Wang, 2019; Steele et al., 2021).

3.3. Sextons: the Martian pseudo-seasons

Based on the observed dust storm distribution (Figs. 3 and 4), it is convenient to divide the Martian year into six *pseudo-seasons* or "*sextons*" (named loosely following Latin numbering as "Unober", "Douber", "Triober", "Quartober", "Quintober", and "Sixtober"). As summarized in Table 1, the six sextons in sequence span a whole Mars year. Although this is only one possible way to partition a Martian year, it is useful in highlighting the characteristics of the statistical distributions of dust storm instances, individual dust storms and dust storm sequences over the annual cycle. The lengths of the sextons vary to best accommodate the similarities within each and the differences among them. Note that the boundaries of the sextons are suggestive, future studies using additional data may help with more useful definitions.

Based on Figs. 3 and 4, we designate the 1st pseudo-season Unober as spanning $L_s = 0°$–$70°$. It mainly includes small sized ($< 5 \times 10^6$ km^2) dust storm instances of individual dust storms following the receding north polar cap and the growing south polar cap, with the southern population occasionally organizing into dust storm sequences that extend to the southern lower latitudes in southern mid-fall.

The 2nd one Douber spans $L_s = 70°$–$135°$ which corresponds approximately to the solstitial pause in the southern hemisphere (Lewis et al., 2016; Hinson and Wilson, 2021). The dust activity is mainly due to the north polar population that resides near the residual north polar cap, especially in the longitudinal sector corresponding to Acidalia or Utopia. While it is unrelated to this paper, Duober is also the sexton uniquely defined by the exposed northern residual ice cap, a thick tropical water ice cloud belt, and peak atmospheric water vapor (e.g., Wang and Ingersoll, 2002; Smith, 2004; Pankine et al., 2013; Wolff et al., 2019; Giuranna et al., 2021).

Triober spans $L_s = 135°$–$185°$ and includes many dust storm instances and individual dust storms with an area $>5 \times 10^6$ km^2 in both hemispheres. The northern population is associated with the formation of the north polar hood and is observed at all longitudes (Fig. 3). The southern population follows the receding south polar seasonal cap, and often organizes into dust storm sequences that extend into the southern low latitudes. The large dust storm sequences originating from the ASV region in MY 29 noticeably influenced the large-scale circulation (Battalio and Wang, 2019), and were referred to as "Z" storms by Heavens et al. (2019) and Steele et al. (2021).

Quartober, the 4th sexton, spans $L_s = 185°$–$245°$ and includes large dust storm episodes which consist of groups of dust storm sequences. These large dust storm episodes can significantly affect the large-scale background dust opacity and global circulation. Kass et al. (2016) previously labeled them as "A" storms based on temperature observations. Most of the dust storm sequences of the large dust storm episodes in Quartober originate from Acidalia or Utopia in the northern hemisphere and later become larger in the southern hemisphere. Previous studies suggest that baroclinic eddies in the vicinity of the north polar vortex are important for triggering flushing dust storms that act as dust storm members of the corresponding dust storm sequences (Wang et al., 2003; Hinson et al., 2012; Greybush et al., 2018; Battalio and Wang, 2020; Hinson and Wilson, 2021).

Quintober, the 5th sexton, spans $L_s = 245°$–$295°$ and corresponds to the solstitial pause in the northern hemisphere winter. Although the dust storm activity is diminished, the background dust opacity is higher than that in the first half of the Mars year. The small individual dust storms at the south polar cap edge near the beginning of Quintober lead to a zonally contiguous elevated background dust around the south polar region. Although limited in area, these polar dust storms lead to a prominent high temperature anomaly at 50 Pa and were referred to as "B" storms in Kass et al. (2016).

Sixtober, the 6th sexton, spans $L_s = 295°$–$360°$ which is characterized by the return of large dust storm episodes after the Quintober pause. These dust storm episodes typically result from dust storm sequences originating from Acidalia or Utopia. Kass et al. (2016) referred to them as "C" storms. Multiple dust storm episodes are observed in Sixtobers of MY 29, 30, and 32, and are discussed further below.

Table 1
Definition of the six pseudo-seasons (referred to as "sextons" by analogy with seasons) based on the observed characteristics of dust storm distributions, along with typical types of dust activity and related names previously published in the literature and commonly used for different aspects of dust storms (see text for details). The (slightly anglicized) names of the pseudo-seasons combine the modified latin numbers 1–6 and the latin *-ber* suffix for "month". We present two options for the name of the 6th sexton, as the more correct version can be somewhat risible for English speakers. The first three (shaded blue) correspond approximately to the half of the year encompassing the aphelion (Ls = 71°) when Mars is further from the sun, and the latter three (shaded red) approximately correspond to the half of the year including the perihelion (Ls = 251°). Although not the topic of this paper, large-scale cloud features as observed in MDGMs are also listed for each sexton. The Ls ranges of sextons are suggestive. The correspondence between the sextons and previous names is approximate, i.e., the borders of the sextons defined here are in some cases slightly different from the borders used in the definitions of previous names.

Pseudo-season (Sexton) Name	Ls Interval	Typical Dust Storm and Cloud Events in MDGMs	Related Name
Unober (1st)	0°-70°	Individual dust storms near both north and south polar caps, occasional noticeable dust storm sequences from southern high latitudes towards southern low latitudes. South polar hood increases, north polar hood decreases.	-
Duober (2nd)	70°-135°	North polar population of individual dust storms, generally quiescent dust activity elsewhere. South polar hood, north polar arc-shaped or spiral clouds, prominent tropical cloud belt.	-
Triober (3rd)	135°-185°	Individual dust storms near both north and south polar caps, occasional large dust storm episodes with southern hemisphere origins. North polar hood formation, south polar hood dissipation.	"Z"
Quartober (4th)	185°-245°	Large dust storm episodes typically originating from the northern hemisphere, dusty background. North polar hood.	"A"
Quintober (5th)	245°-295°	South polar population of individual dust storms, generally quiescent dust activity elsewhere, dusty background. North polar hood.	"B"
Sixtober or Sextober (6th)	295°-360°	Large dust storm episodes typically originating from the northern hemisphere, dusty background. South polar hood formation, north polar hood.	"C"

3.4. Dust storm episodes

3.4.1. Episode occurrence within sextons

Telescopic and early spacecraft observations showed that global dust storms occur roughly every few Mars years during the dust storm season (McKim, 1999; Shirley and Mischna, 2017; Newman et al., 2019), which was described as "episodic" by Zurek and Martin (1993). There was no global dust storm during our study period. However, with the more extensive, nearly continuous monitoring provided by MDGMs, the observed Martian dust storm activity appears to exhibit periods of recurrence on a variety of time scales, giving an impression of loosely connected "episodes" at quasi-periodic intervals.

Figs. 3 and 4 offer a glimpse of the recurrent dust storm activity throughout the year, as multiple dust storm episodes are frequently observed within each sexton. The term *dust storm episode* here refers to a cluster of concurrent or staggered dust storm sequences that collectively result in a large peak in the time series of the daily total storm area over the planet (see the appendix). These dust storm episodes are often associated with a subsequent increase in background dust opacity and significant changes in large-scale circulation. Dust storm episodes are most clearly observed in Sixtober, but are also suggested in Unober, Triober, and Quartober. For example, in Sixtober of MY 32, there were two dust storm episodes, one near $L_s = 315°$ and the other near $L_s = 330°$.

To facilitate the visualization of dust storm episodes in various sextons, Fig. 5 shows the time series of dust storm areas for the sols with MDSSD dust storm sequences. The black line is the total area of all dust storm instances on each sol. The stars mark the apparent peaks. These peaks have areas $>7 \times 10^6$ km^2 (about 5% of the total surface area of Mars) and durations >5 sols. The lines with other colors correspond to the daily total areas of dust storm sequences originating from different regions. The shaded vertical bars indicate the sols with either multiple or merged dust storm sequences. As a reference, the gray line shows the global-mean dust optical depth derived from the Montabone et al. (2015) dust scenarios (right axis).

Fig. 5 shows that all the major peaks of the background dust opacity result from large dust storm episodes in Triober, Quartober, or Sixtober. Many prominent variations in the background dust can also be linked to dust storm episodes immediately preceding them. Dust storm episodes are usually associated with multiple or merged dust storm sequences as indicated by the shading. In other words, these dust storm sequences often work together, resulting in episodic local peaks in the time series of daily total dust storm area.

The combination of Triober and Quartober forms the longest stretch of time with active dust activity during a typical Mars year, which drives a general increase of background dust across this time period. During Triober, the southern hemisphere sequences tend to decrease, and the northern hemisphere sequences increase with time (Figs. 3 and 5). The largest dust storm episode of an average Mars year tends to occur in Quartober. In Sixtober of MY 29, 30, and 32 there were multiple large dust storm episodes of similar size, while in the same sexton of the other two Mars years only a single dominant episode occurred, which was preceded and succeeded by smaller ones. The dust storm episodes in Quartober and Sixtober will be further discussed in Sections 3.4.2 and

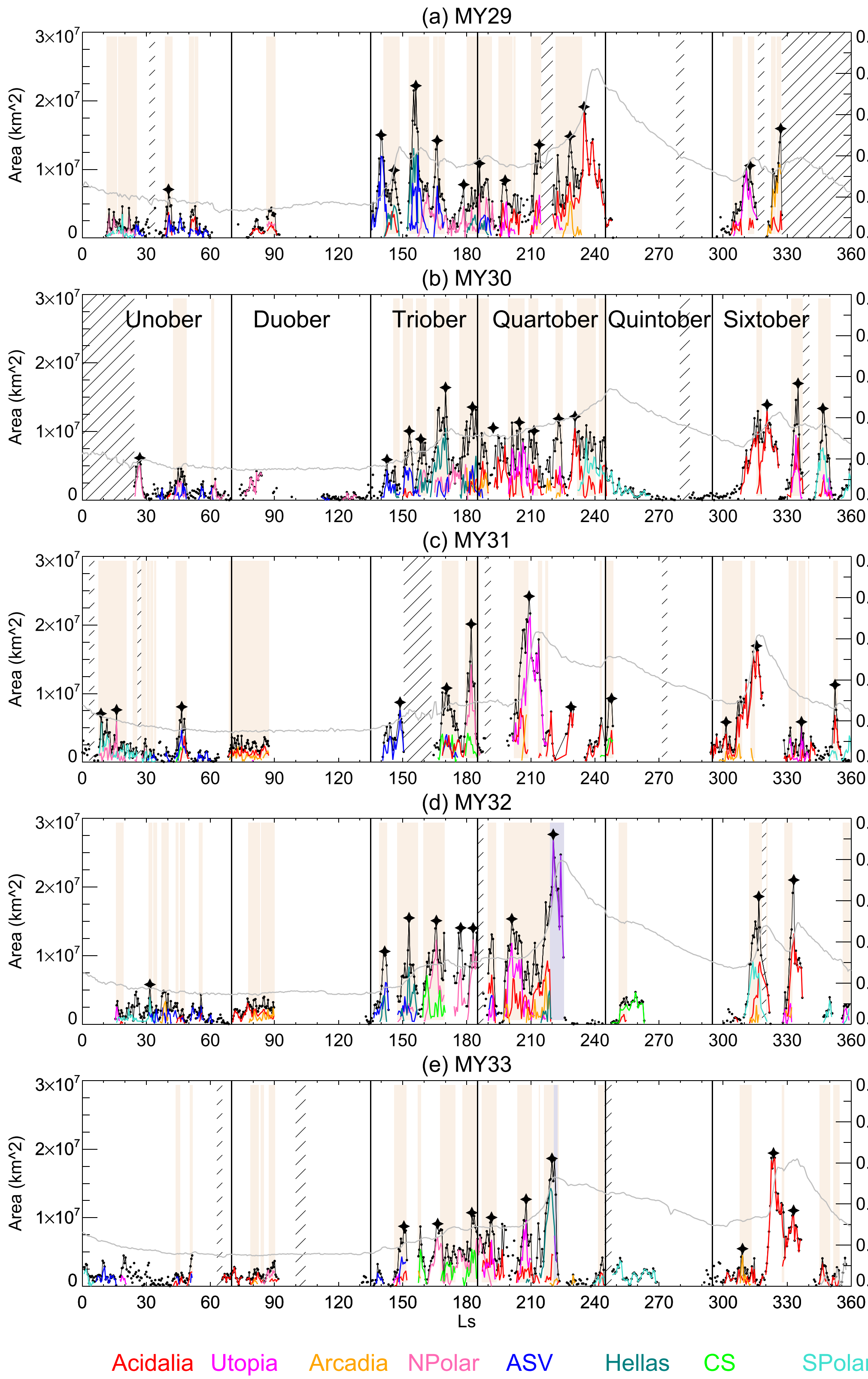

Fig. 5. Time series of the daily total area of dust storm instances in MDGMs for (a-e) MY 29 to 33. The vertical black lines are delimiters of sextons, with the names denoted in Panel (b). The non-vertical black line (left axis) is for the sum of all MDSSD dust storm instances of individual dust storms on each sol. The other colored lines (left axis) represent the MDSSD dust storm members of the corresponding dust storm sequences (legend at the bottom). Shadings indicate the sols with (light brown) multiple or (light purple) merged dust storm sequences. Stars indicate peaks in the black line that are >7 × 10^6 km^2 and longer than 5 sols. Hatches indicate missing MDGMs. The gray line (right axis) is the global-mean dust optical depth derived from the Montabone et al. (2015) dust scenario (scaled to 610 Pa). The time periods with missing MDGMs are indicated by hatch marks. (For interpretation of the references to color in this figure legend, the reader is referred to the web version of this article.)

3.4.3. The individual dust storms in Unober, Duober, and Quintober are generally small in size and limited to the polar regions, and thus they are not discussed further.

A prominent feature, illustrated in Fig. 5, is the quasi-regular time spacing of the peaks in the total dust storm area (black line) for Triober, Quartober and Sixtober. To further illustrate this characteristic, Fig. 6 shows the histogram of the L_S intervals between the adjacent peaks marked by stars in Fig. 5. A bin size of 3° of L_s is used for Fig. 6. The histogram shows a mode around 13° of L_s with a full width at half maximum (FWHM) of about 9° of L_s. The mean, median and standard deviation of the intervals are 13.1°, 12.4° and 4.6°, respectively. Battalio and Wang (2019) noticed a quasi-periodicity near 20 sols (equivalent to about 10° of L_s) for the ASV dust storm sequences in MY 29 and suggested its similarity to the periodicity of the baroclinic annular modes (Battalio and Lora, 2021). We show that such a quasi-periodic recurrence generally applies to the dust storm episodes over the planet in Triober, Quartober and Sixtober during the dust storm season.

3.4.2. *Sixtober episodes*

The spatial extent of the large dust storm episodes observed in Sixtober of MY29–33 is shown in Fig. 7. The color-filled contours superimposed on the base MDGM represent the fraction of sols during each dust storm episode that a dust storm instance exists at the location. The duration of each episode is indicated by the L_s interval shown above each plot. To simplify description in this paper, we give each dust storm episode a name. For example, MY 29 Sixtober-1 refers to the first dust storm episode in Sixtober MY 29 (which occurred at around $L_s = 310°$).

The most common dust activity pattern in these episodes involved flushing through Acidalia from north to south, and is accompanied by dust activity in other areas, such as Utopia, Arcadia, Hellas, and the south polar region (Fig. 7). Under-developed Acidalia dust activity largely remains in the Acidalia general region, e.g., MY 29 Sixtober-2, MY 30 Sixtober-2, MY 30 Sixtober-3. When fully developed, the Acidalia dust activity extends to the southern hemisphere and expands zonally before losing its identity (e.g., MY 30 Sixtober-1, MY 31 Sixtober-1, MY 32 Sixtober-1, MY 32 Sixtober-2, MY 33 Sixtober-1).

The starting L_s (342.9°) of the MY 30 Sixtober-3 episode (Fig. 7e) is the latest among the years studied. The northern hemisphere sequences of this dust storm episode are the least developed. The south polar dust activity is well-separated from that in the northern hemisphere and is involved in the formation of the south polar hood. The south polar hood typically begins to form near $L_s \sim 350°$ to which the MY 30 Sixtober-3 episode is the closest in time. Perhaps this is why the spatial dust distribution resembles that expected for Unober more than the other Sixtober episodes.

The MY 29 Sixtober-1 (Fig. 7a) episode is the earliest in L_s among the episodes shown. Its development history suggests that the dust activity in the Hellas region is due to local dust lifting triggered by earlier dust storm members of a Utopia dust storm sequence. Thus, the dust storm instances in both the Utopia and Hellas regions belong to the Utopia sequence (Fig. 5) even though the dust activity lasts longer and grows larger in the Hellas region. MY 29 Sixtober-1 is the only large dust storm episode in Sixtober that involves Hellas. This behavior of dust activity in the Hellas region being triggered by dust storm members from Utopia is reminiscent of the MY 31 Quartober-1 episode (near $L_s = 210°$, Fig. 5), and probably suggests some similarity in atmospheric dynamics between them. Although the area in Acidalia appears to be connected to the area in Hellas in Fig. 7a, the Acidalia sequence was brief in time (Fig. 5) and remained within the Acidalia region. It contributed to the MY 29 Sixtober-1 episode, but it did not merge with the Utopia sequence.

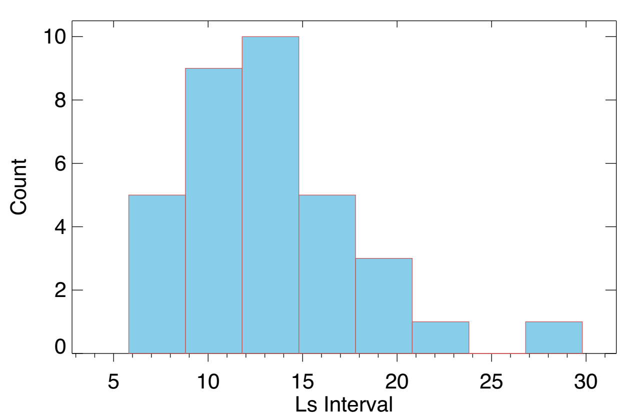

Fig. 6. Histogram of the time interval between adjacent peaks of total dust storm area in Triober, Quartober and Sixtober, as indicated by stars in Fig. 5.

The MY 29 Sixtober-2 episode (Fig. 7b) is initially dominated by an Arcadia sequence (Fig. 5). Unfortunately, its later history cannot be tracked due to missing MDGMs. The MY 32 Sixtober-1 episode (Fig. 7g) mainly includes dust activity in the south polar region and is staggered in time with an Acidalia sequence. The south polar dust activity occurred first and led to a dusty background at the southern high latitudes (Fig. 5). During this period of increasing dustiness, the Acidalia sequence reached the southern high latitudes and dissipated into the dusty background. This type of south polar dust activity normally occurs in Quintober, but in MY 32, it lasted into Sixtober.

3.4.3. *Quartober episodes*

Fig. 5 suggests that the dust activity in Quartober promotes an increase in the background dust opacity, and when a particularly large dust storm episode occurs, a sharp increase in background dust opacity follows. Of the 5 Mars years studied, 3 had the largest dust storm episodes occurring in Quartober. The mean spacing between the peaks of the black curve in Fig. 5 for the Triober and Quartober (12.3° of L_s) is somewhat closer than that for Sixtober (14.6° of L_s), though the difference is within one standard deviation of the overall distribution shown in Fig. 6 (4.6° of L_s).

Fig. 8 shows the spatial coverage of all the MDSSD dust storm instances during $L_s = 200°$–$240°$ for each Mars year and the average of all the years in the study period. The general pattern gives the impression of three longitudinal channels connecting the northern and southern circumpolar zones. The distribution highlights the Acidalia, Utopia, and Hellas regions which are the primary origins of dust storm sequences (Wang and Richardson, 2015; Battalio and Wang, 2021). The differences among the years are related to which channels are more active and in what order.

Almost no dust storm instances were identified in the interiors of Tharsis and Arabia. These regions have high broadband surface albedo and low thermal inertia (Christensen et al., 2001). Although it is more difficult to discriminate dust storms against a bright surface, the absence of dust storms in these regions is most likely not due to the bias related to this difficulty. First of all, in some years, dust storms instances were detected in the peripheries of these regions which have similar albedo as the interiors (Fig. 8), Secondly, surface features are more or less uniformly dark in blue wavelengths (and even reverse contrast in UV wavelengths, i.e., higher red albedo corresponds to lower UV albedo (Wolff et al., 2019)). Thick dust storms are brighter than the surface in these short wavelengths, and if they occur, they would have shown discernable color anomalies in the full-color MDGMs (Wang and Gonzalez Abad, 2021). Thirdly, lack of dust storm instance does not preclude existence of dust haze in the general region.

Quartober MY 30 has the smallest peak in the daily total area time series in Fig. 5. Dust storm sequences were identified in the northern hemisphere, but their dust storm members largely remained within their origination plains (Figs. 3 and 4). Very few individual dust storms occurred near Hellas. Towards the end of Quartober MY 30, south polar dust activity began and continued into Quintober. No particular dust storm episode stands out in this Mars year.

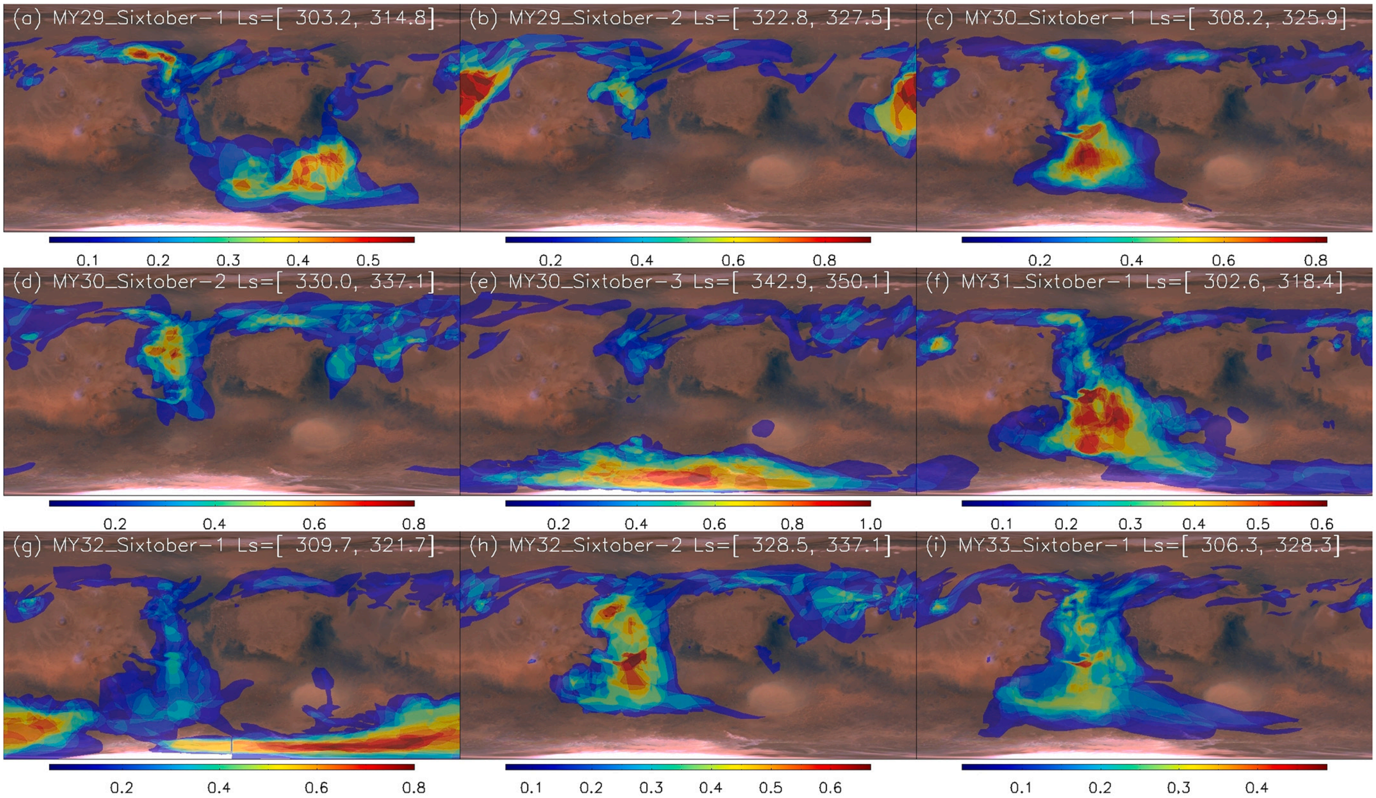

Fig. 7. Dust storm occurrence frequency for the major dust storm episodes in Sixtober MY 29–33. The filled color contours superimposed on the base MDGM represent the fraction of time a pixel is within a dust storm instance during the corresponding L_s period indicated in each panel. The base MDGM indicates surface albedo features and is created by taking the median Data Number (DN) in each color channel at each pixel over all the MDGMs used for this study.

The largest Quartober dust storm episodes in MY 29 and MY 33 are similar in size (Fig. 5), but they exhibit very different development histories. The MY 29 episode ($L_s \sim 235°$) is dominated by an Acidalia sequence (Figs. 4 and 5) that traveled a much longer than usual distance to the southern hemisphere, eventually encircling the south pole from the west to the east. This circumpolar dust activity essentially emulates the role of the regular Quintober south polar dust activity in other Mars years.

In comparison, the MY 33 episode near $L_s \sim 220°$ is dominated by a Hellas sequence, with a minor contribution from an Acidalia sequence (Figs. 4 and 5). A significant Utopia sequence near $L_s \sim 205°$ dominated the previous dust storm episode of this year. However, the Utopia sequence finished before the Hellas sequence started. Had the Utopia and Hellas sequences overlapped in time, Quartober MY 33 would probably have had a larger dust storm episode.

The MY 31 episode near $L_s \sim 210°$ is dominated by a Utopia sequence (Figs. 4 and 5) that crossed the equator and triggered new dust lifting near Hellas (Fig. 9a). At the early stage, there were accompanying Acidalia (Fig. 9b) and Arcadia (Fig. 9c) sequences, which largely remained within their origination plains. This large episode occurred in the first half of Quartober and was followed by a couple of smaller dust storm episodes (Figs. 3-5).

The largest episode in Quartober MY 32 has a peak area of about 2.5 $\times$ 10^7 km^2 and the most complicated development history within the study period (Fig. 5). It started from an Acidalia sequence (Fig. 9d) with an accompanying Arcadia sequence (not shown). Then, dust activity started almost simultaneously in Utopia (not shown) and Hellas (Fig. 9e). Because of missing imaging data, it is not possible to tell if any dust storm members from the Utopia sequence had merged with the Hellas sequence. However, a couple of sols later, the Hellas sequence was observed to merge with the Acidalia sequence, leading to a large area that remained dusty above the background for approximately the next 10° of L_s (Fig. 9f). This process exemplifies the effect of dust storm sequence merger on the development of large dust storm episodes.

3.4.4. *Quasi-periodicity within dust storm sequences*

The quasi-periodicity of dust storm activity can be found in the development histories of individual dust storm sequences. As examples, Fig. 10 shows four representative large dust storm sequences with peak daily total area $> 10^7$ km^2. They were the main contributors to their corresponding dust storm episodes, and were important for the overall dust storm distribution. Each panel is a latitude versus L_s plot of the centroids of the dust storm members of the corresponding dust storm sequence. Each dot represents a dust storm instance and is colored according to its area. Each string of connected dust storm instances indicates a multi-sol dust storm member, and each non-connected dust storm instance is a single-sol individual dust storm.

Fig. 10 shows a classical behavior of large dust storm sequences in Quartober (Panel a, b, d) and Sixtober (Panel c). The behavior is observed for both Acidalia sequences (Fig. 10a, c, d) and Utopia sequences (Fig. 10b). Dust activity generally progresses from the northern mid latitudes to the southern mid-to-high latitudes with time. Early in the sequence lifetime, multiple dust storm members occur on each sol and many last multiple sols. The recurrence characteristics of dust storm sequence activity is manifested by multiple dust storm members propagating southward, many of which are flushing dust storms (Wang et al., 2003). This often occurs in a staggered fashion, with adjacent dust storm members spaced in time quasi-periodically by up to a few sols.

Later in the sequence lifetime, larger dust storm members occur in the southern hemisphere, the dust activity in the northern hemisphere origination region gets reduced or completely stops, fewer number of individual dust storms are observed on each sol. There is eventually a predominant dust storm member that accounts for almost all the sequence area. Battalio and Wang (2020) found that the suppression of

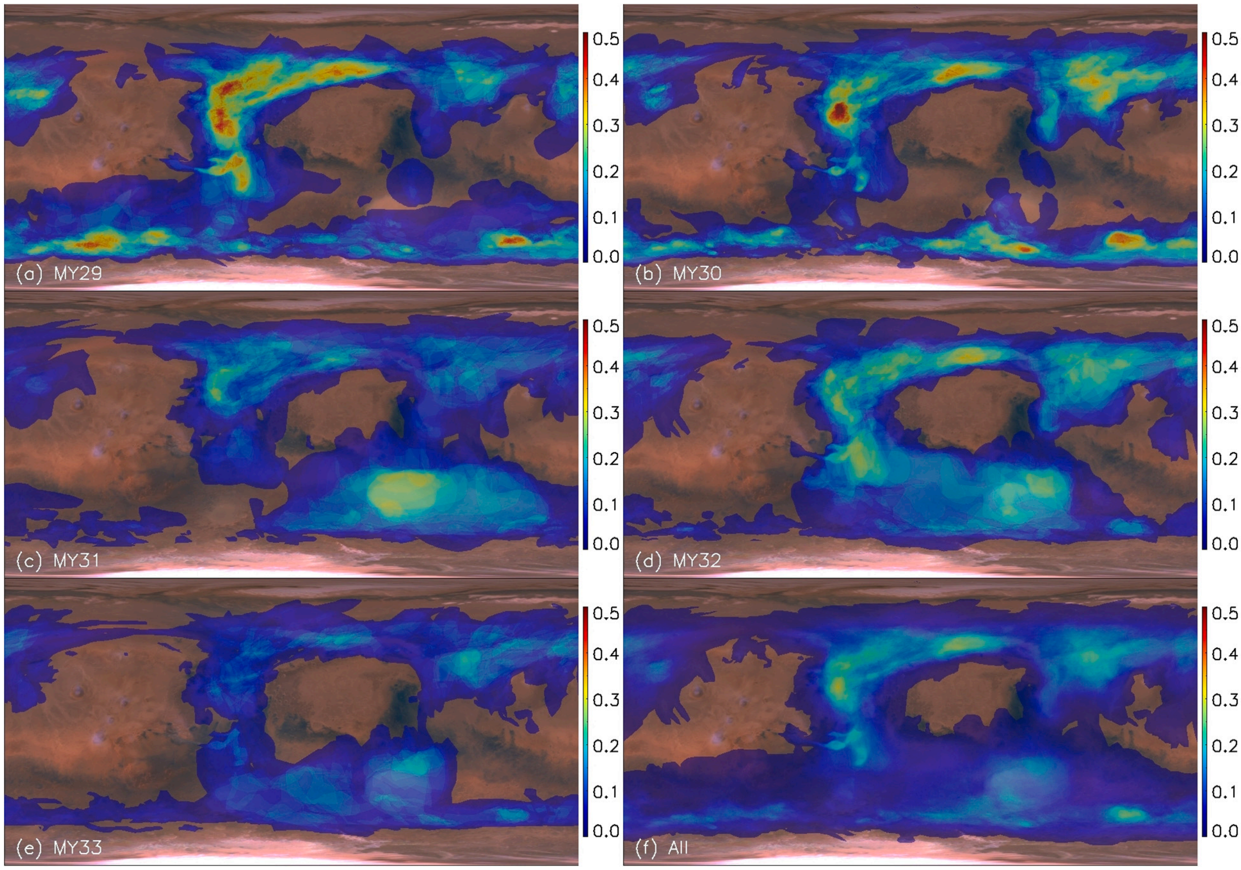

Fig. 8. Dust storm occurrence frequency during $L_S = 200°–240°$ (within Quartober) for (a-e) each year from MY 29 to 33 and (f) average of all years between MY 29 and 33. The filled color contours superimposed on the base MDGM represent the fraction of time a pixel is within a dust storm instance during the time period.

the northern dust activity at the late stage of a large dust storm sequence is associated with weakened 2–8 sol transient eddies and amplified $\leq$1 sol eddies. Furthermore, the fully fledged large dust storm sequences are subsequently followed by transient eddies with long wave periods (>8 sol).

Smaller dust storm sequences in Quartober and Sixtober occur more often than the fully fledged ones discussed above (Fig. 5). These smaller sequences are largely confined to the northern hemisphere and lack the development of large dust storm members in the southern hemisphere. However, the development history in the northern hemisphere also exhibits quasi-periodic recurrence of multiple flushing dust storm members. The difference is that the dust storm members tend not to travel as far southward as those in larger sequences.

4. Summary

Dust storm instances were manually identified using the MRO Mars Daily Global Maps (MDGMs) (Wang and Gonzalez Abad, 2021) from MY 29 to MY 33. Following previous studies (Wang and Richardson, 2015; Battalio and Wang, 2021), each individual dust storm (captured by one or more dust storm instance) was tracked with its storm ID, and when appropriate, was grouped into a dust storm sequence with a sequence ID. The resulting Mars Dust Storm Sequence Dataset (MDSSD) contains >12,000 dust storm instances and >200 dust storm sequences.

The MDSSD was used to investigate dust storm distributions for MY 29–33, none of which had a global dust storm. To capture the annual cycle of the dust activity in a naturally consistent way, we partitioned the Mars year into six climate pseudo-seasons (or “sextons” in analogy with seasons) which we have named “Unober”, “Duober”, “Triober”, “Quartober”, “Quintober”, and “Sixtober”. Each sexton exhibits a characteristic pattern of where and how dust storms occur, though the L_s boundaries are not strict. The combination of Triober through Sixtober approximately spans the conventional dust storm season as defined in Martin and Zurek (1993). Sextons can also be useful for describing most of the seasonal variations of the large-scale water ice clouds observed in MDGMs (see Table 1).

For consistency in describing dust storms, we use the term “dust storm episode” to refer to a noteworthy peak in the time series of daily total dust storm area. These dust storm episodes typically result from a clustering of dust storm sequences that are simultaneous, staggered, or merged. Each dust storm sequence is in turn a collection of dust storm members that appear to follow a general spatial trajectory and form a coherent development history. A dust storm member can be of any size and duration and is an integral part of the corresponding dust storm sequence.

A sexton usually hosts multiple dust storm episodes. The terminology developed here builds upon imaging observations that provide a somewhat different picture of storm behavior from that seen in atmospheric temperature retrievals (Kass et al., 2016). Signals in temperature depend on the size, location, and season of dust storm episodes, and may sometimes be more closely connected with the large-scale dust background which results from dust storm episodes. Furthermore, the temperature signals of smaller dust storm episodes may sometimes be concealed by those of larger episodes.

The overall spatial evolution of dust storm instances within Quartober has striking similarities among the years studied, featuring a northern and a southern mid/high latitude zone with three longitudinal channels. There is also a similarity in the overall spatial distributions for Sixtober. However, within each sexton, the details differ on the trajectories and order of dust storm sequences, which results in vastly different development histories of dust storm episodes.

Martian dust storm distributions consist of a series of loosely

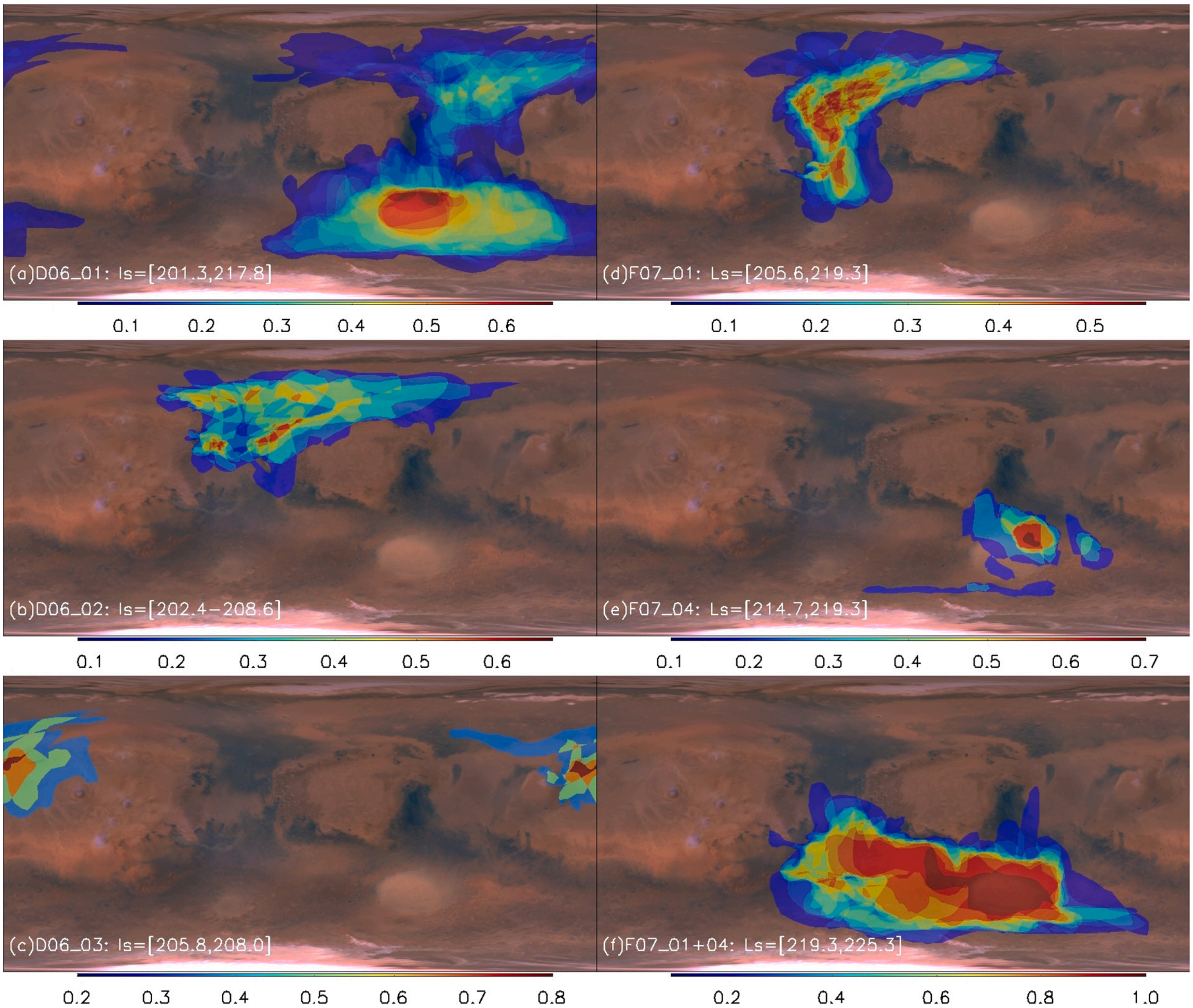

Fig. 9. Dust storm occurrence frequency for corresponding Quartober dust storm sequences. The Sequence ID and L_s range are indicated in the lower left corner of each panel. Individual dust storms not belonging to the corresponding dust storm sequence are not considered. The filled color contours represent the fraction of time a pixel is occupied by a dust storm instance of a dust member during the corresponding L_s period spanned by the dust storm sequence. Panels (a-c) are for three dust storm sequences involved in a dust storm episode in Quartober MY 31. Panels (d-f) are for three dust storm sequences involved in a dust storm episode in Quartober MY 32.

connected components occurring at quasi-periodic intervals. This type of recurrence can be seen in dust storm episodes and within dust storm sequences and is reminiscent of the quasi-periodic occurrence of global dust storms (Zurek and Martin, 1993; McKim, 1999; Shirley and Mischna, 2017).

A classical large dust storm sequence features two distinct development stages. In the first stage, many recurrent dust storm members propagate southward from the northern mid-to-high latitudes. The dust storm members typically last a few sols and are staggered in time, which maintains continuous dust activity in the general region. In the second stage, the dust storm members are fewer in number, larger in area and located in the southern mid-to-high latitudes.

Several caveats are worth mentioning. First, the Montabone et al. (2015) dust optical depth scenarios are convenient to use and offer direct connections with the MDSSD data on a large scale. However, due to extrapolation and representation errors in the Montabone et al. (2015) dust optical depth kriged dataset, some column dust opacity data have low reliability value for the MRO era. This can sometimes lead to large discrepancies with respect to image observations (Montabone et al., 2015). Second, the nature of the MDSSD data makes it difficult to quantify the errors in the measured quantities. Even though a quality flag is employed, data defining an individual dust storm instance's boundary is subjective. Despite this inherent subjectivity, we have strived to present statistically robust results in this paper. We provide the MDSSD on Harvard Dataverse as a guide for users to compare against their own marked objects in MDGMs. Third, while the best available systematic daily global coverage for the study period is provided by MDGMs, the observations are still not frequent enough to ensure confidence in attempting continuous feature tracking. Future missions providing such a capability, such as from satellites in areo-synchronous orbit, are needed to fill this gap (Montabone et al., 2021).

Finally, the terminology in this paper is offered as an orderly alternative to other existing terminology. It is useful for organizing the information extracted from MDGMs and for highlighting the multiple levels of recurrence of Martian dust storms in a hierarchical way. This terminology is therefore process oriented. In comparison, the traditional terminology (local, regional, etc.) is oriented towards individual dust storm parameter (size and/or duration), and the alphabetical terminology ("A", "B", etc.) is oriented towards the response to dust perturbation. The sexton terminology may provide some empirical expectation. For example, if there is a Quratober-1 dust storm episode near $L_s = 200°$, then a few other dust storm episodes may be expected to follow later in Quartober; A Quartober episode would most likely involve dust storm sequences through Acidalia and Utopia with

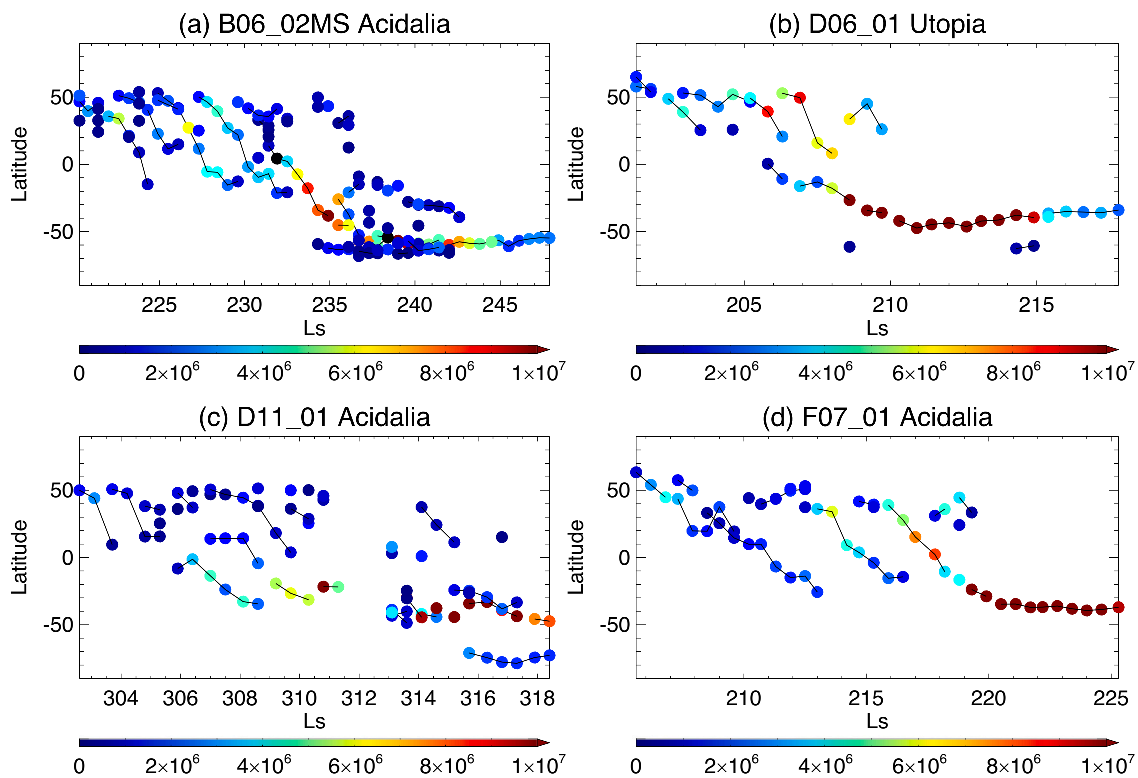

Fig. 10. Latitude versus L_S evolution of large dust storm sequences (a) Acidalia sequence "B06_02MS", (b) Utopia sequence "D06_01", (c) Acidalia sequence "D11_01", and (d) Acidalia sequence "F07_01". Each circle represents a dust storm instance and is colored according to the corresponding area (km^2). Dots connected by solid lines share common storm IDs and represent multi-sol dust storm members. Nonconnected dots represent individual dust storms not trackable for longer than 1 sol.

recurrent flushing dust storm members, and if the episode grows large enough, it could probably trigger or merge with dust activity near Hellas. After identifying sexton seasonal behavior and the episodic nature on multiple levels of dust storm development, future work can advance our understanding by discovering the underlying processes that generate those seasonality and characteristics.

Declaration of Competing Interest

None.

Data availability

The data are publically available and the dois are included in the paper. The MRO MDGMs are available at Harvard Dataverse (https://doi.org/10.7910/DVN/U3766S/). The MGS MDGMs are available at Harvard Dataverse (https://doi.org/10.7910/DVN/WWRT1V). The MDAD v1.0 is available at Harvard Dataverse (https://doi.org/10.7910/DVN/F8R2JX). The MDSSD is available at Harvard Dataverse (https://doi.org/10.7910/DVN/0XB6KN). The Montabone et al. (2015) dust optical depth climatology is available at http://www-mars.lmd.jussieu.fr/mars/dust_climatology.

Acknowledgement

Production of MDGMs was supported by NASA PDART grant #80NSSC20K1056. MDSSD and the analysis in this paper was supported by NASA SSW grant #80NSSC21K1831. MDAD v1.0 was supported by NASA MDAP grant #80NSSC17K0475. M. Saidel's participation in this project was supported by the SAO REU program which was funded in part by the National Science Foundation REU and Department of Defense ASSURE programs under NSF Grant no. AST-1852268. We thank Luca Montabone and an anonymous reviewer for providing thoughtful reviews to improve this paper.

Appendix A. Appendix

We present here a glossary of the terms used in this manuscript for easy reference.

Dust Storm Instance: We define a "dust storm instance" to be an individual cloud of dust as observed in a single MDGM. The "instance" is the dust cloud as imaged at one moment in time. Since a dust storm instance is defined to be a snapshot of an individual dust storm, it contains no information about the time evolution of the storm. The dust storm instance is the simplest *observational* "atomic" unit of the MDSSD dataset.

Individual Dust Storm: We define an "individual dust storm" to be an individual cloud of dust that has been captured in MDGM images over one or more consecutive sols. As such, an "individual dust storm" is comprised of one or more "dust storm instances" in the MDSSD dataset. If the "individual dust storm" consists of only one "dust storm instance", then the instance has a unique dust storm identification number (Storm ID). If the individual dust storm consists of several instances over consecutive sols, then the collection of dust storm instances corresponding to the individual dust storm are all labeled with the same Storm ID. Since it is most common to conceptualize a "dust storm" as an individual cloud of dust that persists in the atmosphere for a finite interval of time, the "individual dust storm" is the element of the MDSSD that is closest to this intuitive definition of an individual dust storm cloud. Similarly, if an "individual dust storm" is thought of as a movie covering the lifetime of an individual dust cloud, then each "dust storm instance" is a frame in that movie. Note that an individual dust storm keeps its identity (Storm ID) throughout its lifetime. An individual dust storm can be of any size and duration. In the MDSSD, a new Storm ID is assigned on the first sol that a new individual dust storm is identified in a MDGM. If the individual dust storm persists in subsequent MDGMs, the same Storm ID is carried across those subsequent dust storm instances. If the individual dust storm cannot be identified on the next sol, then the Storm ID will not be used again in MDSSD. Thus, a Storm ID is equivalent to a Lagrangian tracer for an individual dust storm. While identification of dust storm instances can be done using a single image, identification of an individual dust storm requires a time series of images. Some individual dust storms may only have been observed in one frame of the time series, while other individual dust storms were observed in multiple frames.

Dust Storm Member: While some individual dust storms exist in isolation, many are observed to form and dissipate in a spatial and/or temporal relationship with other individual dust storms. If we find these relationships within the dataset, we define a "dust storm sequence" (see below). A "dust storm member" is then defined to be an individual dust storm that is part of this larger sequence. Thus, "dust storm members" are a subset of the family of "individual dust storms." Note that this definition of dust storm member is slightly different from that used in Battalio and Wang (2021).

Dust Storm Sequence: We define a dust storm sequence as an organization of dust storm members that occur close enough in time and/or space to each other such that they maintain a coherent spatial trajectory and temporal development history. Observationally, a dust storm sequence can only be identified from the evolution evidenced in a timeseries of images and cannot be determined on the basis of a single image. When a collection of "individual dust storms" are found to collectively constitute a "dust storm sequence", each of the "individual dust storms" becomes a member of the sequence and is given an additional Sequence ID in addition to their Storm ID. The Sequence ID is the same for all members of the same sequence. In the MDSSD, a dust storm member has both a Storm ID and a Sequence ID, while an isolated individual dust storm only has a Storm ID.

Dust Storm Episode: A "dust storm episode" is the largest superset of emerging storm behavior discussed in this paper. Dust storm episodes are typically identified by the presence of a large peak in the time series of the daily total storm area over the whole planet. In this paper, a dust storm episode is defined as having a peak area larger than 7×10^6 km^2 (roughly 5% of the total planetary surface area) and a duration of -longer than 5 sols. In the very largest of dust events, the increase in atmospheric dust opacity is often associated with the action of concurrent or consecutive dust storm sequences. These may be sequences that occur in different regions but appear to interact, or they may be other parallel occurrence of sequences that cumulatively elevate the atmospheric dust opacity.

Pseudo-Seasons or "Sextons": Dust storm (and other climate) behavior suggests a division of the Martian year into six variable duration intervals. We coin the term "sexton" for each of these intervals, in a simplistic analogy with the terrestrial month. In practice, seasonal groupings of months (like June–July-August, or JJA) are often used in terrestrial climate science, and the sextons defined here are perhaps most directly analogous with those. However, instead of being based on the Martian orbit, sextons are defined from the outset as intervals within which there are similar patterns of dust storm behavior, and between which the behavior can be quite different. Specifically, the boundaries, though not strict, are defined in terms of distinct behavior of dust storm activity. As dust is a major factor in the Martian climate, sextons can also help categorize and describe the climate system as a whole, including separating intervals of distinct behavior of large-scale water ice cloud features. More details are provided in Table 1.

Appendix B. Supplementary data

Supplementary data to this article can be found online at https://doi.org/10.1016/j.icarus.2022.115416.

References

Barnes, J.R., Haberle, R.M., Wilson, R.J., Lewis, S.R., Murphy, J.R., Read, P.L., 2017. The global circulation. In: Atmosphere and Climate of Mars. Cambridge Planetary Science Series, pp. 229–294.

Battalio, J.M., Lora, J., 2021. Annular modes of variability in the atmospheres of Mars and titan. Nat. Astron. 5 (11), 1139–1147. https://doi.org/10.1038/s41550-021-01447-4.

Battalio, J.M., Wang, H., 2019. The Aonia-Solis-Valles dust storm track in the southern hemisphere of Mars. Icarus 321, 367–378. https://doi.org/10.1016/j.icarus.2018.10.026.

Battalio, J.M., Wang, H., 2020. Eddy evolution during large dust storms. Icarus 338. https://doi.org/10.1016/2019.113507.

Battalio, J.M., Wang, H., 2021. The Mars dust activity database (MDAD): a comprehensive statistical study of dust storm sequences. Icarus 354. https://doi.org/10.1016/j.icarus.2020.114059.

Bell III, J.F., Wolff, M.J., Malin, M.C., Calvin, W.M., Cantor, B.A., Caplinger, M.A., Clancy, R.T., Edgett, K.S., Edwards, L.J., Fahle, J., Ghaemi, F., Haberle, R.M., Hale, A., James, P.B., Lee, S.W., McConnochie, T., Noe Dobrea, E., Ravine, M.A., Schaeffer, D., Supulver, K.D., Thomas, P.C., 2009. J. Geophys. Res. 114, E08S92 https://doi.org/10.1029/2008JE003315. Mars Reconnaissance Orbiter Mars Color Imager (MARCI): Instrument description, calibration, and performance.

Cantor, B.A., 2007. MOC observations of the 2001 Mars planet-encircling dust storm. Icarus 186, 60–96.

Cantor, B.A., James, P.B., Caplinger, M., et al., 2001. Martian dust storms: 1999 Mars orbiter camera observations. J. Geophys. Res. 106 (E10), 23653–23687. https://doi.org/10.1029/2000JE001310.

Christensen, P.R., Banfield, J.L., Hamilton, V.E., Ruff, S.W., Kieffer, H.H., Titus, T.N., Malin, M.C., Morris, R.V., Lane, M.D., Clark, R.L., Jakosky, B.M., Mellon, M.T., Pearl, J.C., Conrath, B.J., Smith, M.D., Clancy, R.T., Kuzmin, R.O., Roush, T., Mehall, G.L., Gorelick, N., Bender, K., Murray, K., Dason, S., Greene, E., Silverman, S., Greenfield, M., 2001. Mars global surveyor thermal emission spectrometer experiment: investigation description and surface science results. J. Geophys. Res. 106 (E10), 23823–23871.

Giuranna, M., Wolkenberg, P., Grassi, D., Aronica, A., Aoki, S., Scaccabarozzi, D., Saggin, B., Formisano, V., 2021. The current weather and climate of Mars: 12 years of atmospheric monitoring by the planetary Fourier spectrometer on Mars express. Icarus 353. https://doi.org/10.1016/j.icarus.2019.113406.

Greybush, S.J., Gillespie, H.E., Wilson, R.J., 2018. Transient eddies in the TES/MCS ensemble Mars atmosphere reanalysis system (EMARS). Icarus. https://doi.org/10.1016/j.icarus.2018.07.001.

Guzewich, S.D., Toigo, A.D., Wang, H., 2015. Mars orbiter camera climatology of textured dust storms. Icarus 258, 1–13. https://doi.org/10.1016/j.icarus.2015.06.023.

Guzewich, S.D., Toigo, A.D., Wang, H., 2017. An investigation of dust storms observed with the Mars color imager. Icarus 289, 199–213. https://doi.org/10.1016/j.icarus.2017.02.020.

Heavens, N.G., Kass, D.M., Shirley, J.H., Piqueux, S., Cantor, B.A., 2019. An observational overview of dusty deep convection in Martian dust storms. J. Atmos. Sci. 76 (11), 3299–3326. https://doi.org/10.1175/jas-d-19-0042.1.

Hinson, D.P., Wilson, R.J., 2021. Baroclinic waves in the northern hemisphere of Mars as observed by the MRO Mars climate sounder and the MGS thermal emission spectrometer. Icarus. https://doi.org/10.1016/j.icarus.2020.114152.

Hinson, D.P., Wang, H., Smith, M.D., 2012. A multi-year survey of dynamics near the surface in the northern hemisphere of Mars: short-period baroclinic waves and dust storms. Icarus 219, 307–320. https://doi.org/10.1016/j.icarus.2012.03.001.

Kahre, M.A., Murphy, J.R., Newman, C.E., Wilson, R.J., Cantor, B.A., Lemmon, M.T., Wolff, M.J., 2017. In: Haberle, R.M., Clancy, R.T., Forget, F., Smith, M.D., Zurek, R. W. (Eds.), The Mars dust cycle. book chapter in Atmosphere and Climate of Mars, pp. P295–P337.

Kass, D.M., Kleinböhl, A., McCleese, D.J., Schofield, J.T., Smith, M.D., 2016. Interannual similarity in the Martian atmosphere during the dust storm season. Geophys. Res. Lett. 43, 6111–6118. https://doi.org/10.1002/2016GL068978.

Kulowski, L., Wang, H., Toigo, A.D., 2017. The seasonal and spatial distribution of textured dust storms observed by Mars global surveyor Mars orbiter camera. Adv. Space Res. 59, 715–721. https://doi.org/10.1016/j.asr.2016.10.028.

Lewis, S.R., Mulholland, D.P., Read, P.L., Montabone, L., Wilson, R.J., Smith, M.D., 2016. The solsticial pause on Mars: 1. A planetary wave reanalysis. Icarus 264, 456–464. https://doi.org/10.1016/j.icarus.2015.08.039.

Liu, J., Richardson, M.I., Wilson, R.J., 2003. An assessment of the global, seasonal and interannual spacecraft record of Martian climate in the thermal infrared. J. Geophys. Res. 108 https://doi.org/10.1029/2002JE001921. E8, Art. No. 5098.

Malin, M., Bell III, J.F., Calvin, W., Clancy, R.T., Haberle, R.M., James, P.B., Lee, S.W., Thomas, P.C., Caplinger, M.A., 2001. The Mars color imager (MARCI) on the Mars climate orbiter. J. Geophys. Res. 106, 17651–17672. https://doi.org/10.1029/1999JE001145.

Martin, J.J., Zurek, R.W., 1993. An analysis of the history of dust activity on Mars. J. Geophys. Res. 98 (E2), 3221–3246. https://doi.org/10.1029/92JE02937.

Martinez-Alvarado, O., Montabone, L., Lewis, S.R., Moroz, I.M., Read, P.L., 2009. Transient teleconnection event at the onset of a planet-encircling dust storm on Mars. Ann. Geophys. 27, 3663–3676.

McKim, R., June 1999. Telescopic Martian Dust Storms: A Narrative and Catalogue, BAA. ISBN 0-902749-13-7,.

Montabone, L., Forget, F., Millour, E., Wilson, R.J., Lewis, S.R., Cantor, B., Kass, D., Kleinbohl, A., Lemmon, M.T., Smith, M.D., Wolff, M.J., 2015. Eight-year climatology of dust optical depth on Mars. Icarus 251, 65–95. https://doi.org/10.1016/j.icarus.2014.12.034.

Montabone, L., Heavens, N., et al., 2021. Observing Mars from Areostationary orbit: benefits and applications. Bull. AAS 53 (4). https://doi.org/10.3847/25c2cfeb.0cdca220.

Newman, C.E., Lee, C., Mischna, M., Richardson, M., Shirley, J., 2019. An initial assessment of the impact of postulated orbit-spin coupling on Mars dust storm variability in fully interactive dust simulations. Icarus 317, 649–668. https://doi.org/10.1016/j.icarus.2018.07.023.

Pankine, A.A., Tamppari, L.K., Banfield, J.L., McConnochie, T.H., Smith, M.D., 2013. Retrieval of martian atmospheric opacities from MGS TES nighttime data. Icarus 226, 708–722. https://doi.org/10.1016/j.icarus.2013.06.024.

Shirley, J.H., Mischna, M.A., 2017. Orbit-spin coupling and the interannual variability of global-scale dust storm occurrence on Mars. Planet. Space Sci. 139, 37–50. https://doi.org/10.1016/j.pss.2017.01.001.

Smith, M.D., 2004. Interannual variability in TES atmospheric observations of Mars during 1999–2003. Icarus 167 (1), 148–165.

Smith, M.D., 2008. Spacecraft observations of the Martian atmosphere. Annu. Rev. Earth Planet. Sci. 36, 191–219. https://doi.org/10.1146/annurev.earth.36.031207.124334.

Steele, L.J., Kleinböhl, A., Kass, D.M., 2021. Observations of ubiquitous nighttime temperature inversions in Mars tropics after large-scale dust storms. Geophys. Res. Lett. 48, 9. https://doi.org/10.1029/2021GL092651.

Wang, H., Gonzalez Abad, G., 2021. Cloud masks derived from the Mars daily global maps and an application to the tropical cloud belt on Mars. Geosciences 11, 324. https://doi.org/10.3390/geosciences11080324.

Wang, H., Ingersoll, A.P., 2002. Martian clouds observed by Mars global surveyor Mars orbiter camera. JGR_planets 107 (E10), 5078. https://doi.org/10.1029/2001JE001815.

Wang, H., Richardson, M.I., 2015. The origin, evolution, and trajectory of large dust storms on Mars during Mars years 24-30 (1999-2011). Icarus 251, 112–127. https://doi.org/10.1016/j.icarus.2013.10.033.

Wang, H., Richardson, M.I., Wilson, R.J., Ingersoll, A.P., Zurek, R.W., 2003. Cyclones, tides, and the origin of major dust storms on Mars. GRL 30 (9), 1488. https://doi.org/10.1029/2002GL016828.

Wolff, M.J., Clancy, R.T., Kahre, M.A., Haberle, R.M., Forget, F., Cantor, B.A., Malin, M. C., 2019. Mapping water ice clouds on Mars with MRO/MARCI, 332, 24–49. https://doi.org/10.1016/j.icarus.2019.05.041.

Zurek, R.W., Martin, L.J., 1993. Interannual variability of planet-encircling dust storms on Mars. J. Geophys. Res. 98 (E2), 3247–3259.

Zurek, R.W., Smrekar, S.E., 2007. An overview of the Mars reconnaissance orbiter (MRO) science mission. J. Geophys. Res. 112, E05S01 https://doi.org/10.1029/2006JE002701.